Published in final edited form as:
Osteoarthritis Cartilage. 2010 January ; 18(1): 88–96. doi:10.1016/j.joca.2009.11.006.

Phenotypic characterization of epiphycan-deficient and epiphycan/biglycan double-deficient mice

Satoshi Nuka, MD[§,*,+], **Wei Zhou, MSc**[§,*,#], **Stephen P. Henry, PhD**[§,*,¤], **Christi M. Gendron, PhD**[§,*], **Jason B. Schultz, BSc**[§,*], **Tamayuki Shinomura, PhD**[§,¶], **Jan Johnson, PhD**[§,^], **Ying Wang, MD**[‡], **Douglas R. Keene, MSc**[ʃ], **Ramiro Ramírez-Solis, PhD**[§,✦], **Richard R. Behringer, PhD**[‡], **Marian F. Young, PhD**[◇], and **Magnus Höök, PhD**[§,**]

[§] Texas A&M University System Health Science Center, Albert B Alkek Institute of Biosciences and Technology, Center for Extracellular Matrix Biology, 2121 W. Holcombe Boulevard, Houston, TX 77030

[◇] Craniofacial and Skeletal Diseases Branch, NIDCR, National Institutes of Health, Bethesda, MD 20892

[ʃ] Shriners Hospital for Children, Portland, OR 97239

[‡] Department of Molecular Genetics, The University of Texas M.D. Anderson Cancer Center, Houston, TX 77030

Abstract

Objective—To characterize the *in vivo* role epiphycan (Epn) has in cartilage development and/or maintenance.

Methods—*Epn*-deficient mice were generated by disrupting the *Epn* gene in mouse embryonic stem cells. *Epn*/biglycan *(Bgn)* double-deficient mice were produced by crossing *Epn*-deficient mice with *Bgn*-deficient mice. Whole knee joint histological sections were stained using van Gieson or Fast green/Safranin-O to analyze collagen or proteoglycan content, respectively. Microarray analysis was performed to detect gene expression changes within knee joints.

Results—*Epn*-deficient and *Epn/Bgn* double-deficient mice appeared normal at birth. No significant difference in body weight or femur length was detected in any animal at one month of age. However, nine-month *Epn/Bgn* double-deficient mice were significantly lighter and had significantly shorter femurs than wild type mice, regardless of gender. Male *Epn*-deficient mice also had significantly shorter femurs than wild type mice at nine months. Most of the deficient

[**]To whom correspondence and reprint requests should be addressed: Dr. Magnus Höök, Telephone: (713)677-7552, Fax: (713)677-7576, mhook@ibt.tamhsc.edu.
[*]Dr. Nuka, Dr. Henry, Ms. Zhou, Dr. Gendron, and Mr. Schultz contributed equally to this work
[+]Present address: Department of Orthopedic Surgery, Hakodate Goryokaku Hospital, Goryokakucho 38-3, Hakodateshi, Hokkaido, Japan
[¤]Present address: Department of Molecular Genetics, The University of Texas M.D. Anderson Cancer Center, Houston, TX 77030
[#]Present address: Genentech, Inc., South San Francisco, CA 94080
[✦]Present address: Wellcome Trust Sanger Institute, Wellcome Trust Genome Campus, Hinxton, Cambridgeshire, UK CB10 1SA
[¶]Present address: Department of Hard Tissue Engineering, Tokyo Medical and Dental University, Tokyo, Japan
[^]Present address: Puget Sound Blood Center, Seattle, WA 98104

CONFLICT OF INTEREST STATEMENT
No conflicts of interests are associated with this manuscript.

animals developed osteoarthritis (OA) with age; the onset of OA was observed earliest in *Epn/Bgn*-double deficient mice. Message RNA isolated from *Epn/Bgn* double-deficient knee joints displayed increased matrix protein expression compared with wild type mice, including other small leucine-rich proteoglycan (SLRP) members such as asporin, fibromodulin, and lumican.

Conclusion—Similar to other previously studied SLRPs, Epn plays an important role in maintaining joint integrity. However, the severity of the OA phenotype in the *Epn/Bgn* double-deficient mouse suggests a synergy between these two proteins. These data are the first to show a genetic interaction involving class Iand class III SLRPs *in vivo*.

Keywords

Osteoarthritis; cartilage; mouse; microarray; small leucine rich proteoglycans

INTRODUCTION

Epiphycan, a chondroitin/dermatan sulfate proteoglycan preferentially expressed in epiphyseal cartilage during embryonic development [1], is a member of the small leucine-rich proteoglycan (SLRP) family. SLRPs are extracellular matrix (ECM) molecules that contain a tandem array of leucine-rich repeat (LRR) motifs flanked by N- and C- terminal cysteines. Many SLRP core proteins are also substituted with glycosaminoglycan (GAG) chain(s), although the presence, nature, and size of the GAGs appear to be tissue-specific and age-dependent [2].

SLRPs are divided into three classes based upon the spacing of their N-terminal cysteines, the number of LRRs they contain, and their corresponding gene structures. Class I (decorin, biglycan, and asporin) and class II SLRPs (fibromodulin, PRELP, keratocan, lumican, and osteoadherin/osteo-modulin) contain 10–12 LRRs, whereas class III SLRPs (epiphycan/PG-Lb/DSPG3, opticin, and osteoglycin/mimecan) contain 6–8 LRRs. Chondroadherin, NYX/nyctalopin, ECM2, podocan, and nephrocan contain both the N-terminal cysteine cluster and the LRR domain characteristics of SLRPs but are not assigned to a class.

SLRPs interact with a variety of ECM proteins. Reported binding partners include fibronectin [3], thrombospondin [4], fibrinogen [5], heparin cofactor II [6], C1q [7–9], mannose-binding lectin [10], collectin 43 [10], conglutinin [10], pulmonary surfactant D [11], and TGF-β [12,13]. The most commonly reported binding partner for SLRP proteins is collagen [14]. Moreover, the targeted disruption of individual SLRPs can lead to obvious collagen fibril formation defects *in vivo*. However, single SLRP-deficient mice display relatively mild phenotypes when considering their tissue distributions; an observation that suggests some SLRPs may compensate for the loss of others. For example, lumican-null mice exhibit corneal clouding and skin laxity, but do not show significant alterations in tendon stiffness [15]. However, lumican loss-of-function enhances the reduced tendon stiffness seen in fibromodulin-null mice, suggesting that lumican compensates for the loss of fibromodulin [16]. This putative genetic interaction is particularly interesting in light of the fact that fibromodulin and lumican bind to a similar site on collagen [17].

Many different SLRPs are expressed in cartilage, including asporin, biglycan, chondroadherin, decorin, epiphycan, fibromodulin, keratocan, lumican, opticin, and PRELP [18–23]. However, the ability of SLRPs to influence OA progression is not understood. Furthermore, increased SLRP degradation has been detected in human osteoarthritic cartilage samples [24]. Such degradation presumably leads to cartilage matrix destabilization. Recent reports have implicated one particular SLRP, asporin, with hip and knee OA in Asian populations [25,26]. A specific human polymorphism in the asporin gene,

resulting in an N-terminal region that contains 14 aspartic acid residues rather than 13 aspartic acid residues, is significantly associated with individuals that have OA.

Very little is reported about class III SLRPs, particularly epiphycan. Epiphycan (*Epn*) expression appears to be restricted to cartilage and testis [27]. The unique tissue expression of *Epn* in chick [28] and mouse [27] cartilage suggests that this SLRP may play a key role in chondrocyte differentiation and, hence, cartilage stability. To further investigate this possibility, we generated and characterized *Epn*-deficient mice. These mice exhibit a very mild skeletal phenotype. Since biglycan (*Bgn*) is also expressed in mouse cartilage, and may compensate for the loss of *Epn*, *Epn/Bgn* double-deficient animals were also generated and characterized.

MATERIALS AND METHODS

Generation of Epn-deficient and Epn/Bgn double-deficient mice

An 8 kb fragment of the 129S6 mouse *Epn* gene was identified with a rat Epn probe and used to construct the targeting vector, which contained a *LacZ* expression cassette followed by a neomycin *(neo)*-resistance gene flanked by loxP sites. A MC-1 *thymidine kinase* cassette was included immediately outside the homologous mouse sequence of the targeting vector.

Mouse AB2.2 embryonic stem cells (ESC; a gift from Allan Bradley) were electroporated with the linearized targeting vector described above using a BioRad Gene Pulser and grown in M15 media containing G418 to select for cells containing the *neo*-resistance gene. The targeting vector was designed to insert the *LacZ* cassette six base pairs downstream of and in frame with the starting ATG codon. ES clones containing the correct insertion were identified by Southern blot hybridization and injected into C57BL/6J albino blastocysts according to standard procedures. High percentage coat-color-contribution chimaeras were crossed with C57BL/6J albino mice to obtain germline transmission of the targeted allele. Southern blot and PCR analyses were used to genotype the mice.

Double heterozygous *Epn/Bgn* mice (F_1 generation) were produced by intercrossing homozygous *Bgn*-deficient females ($Epn^{+/+}Bgn^{-/-}$) with homozygous *Epn*-deficient males ($Epn^{-/-}Bgn^{+/0}$). The production and characterization of *Bgn*-deficient mice was previously described [29]. *Epn/Bgn* knockout mice (F_2) were obtained by intercrossing F_1 double heterozygous *Epn/Bgn* mice. All of the mice were maintained in a hybrid 129S6:C57BL/6J albino genetic background. Each animal experiment was approved by the Institute of Biosciences and Technology Institutional Animal Care and Use Committee.

Southern blot analysis

Mouse ESC genomic DNA was digested with ScaI or BglII. Southern blot hybridization was performed according to the procedure of Ramírez-Solis *et al.* [30] with radiolabeled 5’ or 3’ probes that hybridized to regions of the *Epn* gene lying outside of the targeting vector homology.

PCR

The PCR scheme for the *Bgn* allele was performed as described previously [29]. To identify the *Epn* genotype of each mouse, the following primers were used in separate PCR reactions: a forward primer (Epn1fw) corresponding to sequences in *Epn* exon II (5′-GGTCAGGGGCAAATACCAAGGACTCT), a reverse primer (Epn2rv) corresponding to sequences in *Epn* exon III (5′-CTCTACATGG TTGTCAGGAATGTG), and a second forward primer (Bpa) corresponding to a sequence contained within the bovine growth

hormone polyadenylation signal sequence of the *neo* cassette (5′-GCTTCTGAGGCGGAAAGAACCAGCTA). The amplified PCR product for the wild type *Epn* allele with primer pair Epn1fw/Epn2rv was 2.6 kb, whereas the product for the disrupted *Epn* allele with primer pair Bpa/Epn2rv was 0.4 kb.

Body weight and femur length determination

The body weights and femur lengths of each mouse was measured at one and nine months of age. Femur length was measured under a dissecting microscope using calibers. The data from 13–40 different mice per genotype of each gender were analyzed using the Kruskal-Wallis test followed by a Dunn's multiple comparison post-test.

Histological and Immunohistochemical staining

All tissues were fixed in either 4% paraformaldehyde or 10% formalin, decalcified at room temperature in 0.5M EDTA for ≥ one week, dehydrated in ascending concentrations of alcohol, and paraffin-embedded. Serial sections were cut from the paraffin block using a microtome and thereafter dewaxed and rehydrated. For histological analysis of collagen content, tissue sections were stained with hematoxylin for 2 min followed by immersion in van Gieson stain for 5 min. Remaining sections were stained with hematoxylin for 2 min, briefly differentiated in acidified alcohol, and stained with 0.2% Fast green for 2 min. After washing with 1% acetic acid, the sections were stained with Safranin-O for 3 min to examine tissue morphology and proteoglycan content.

Immunohistochemical staining was performed using polyclonal antibodies that detect either mouse Bgn (LF-159) or mouse Epn (R561). The rabbit polyclonal anti-Bgn antibody, LF-159 [31], was a gift from Dr. Larry Fisher (NIH/NIDCR, Bethesda, MD). The polyclonal anti-Epn antibody, R561, was raised in rabbits against purified recombinant Epn protein (Ala_{18}-Thr_{111} fused at the C-terminus to glutathione S-transferase; Alpha Diagnostics International, San Antonio, TX). R561 antibody characterization demonstrated that it is specific for Epn. Tissue sections were digested with 4 mg/ml hyaluronidase in phosphate buffered saline (PBS) at 37°C for 30 min prior to immunostaining. The sections were then incubated with R561 (1:1000) or LF-159 (1:2000) overnight at 4°C. Antibody-staining was visualized with the Vectastain Elite ABC immunoperoxidase kit (Vector Laboratories, Hercules, CA). Hematoxylin was used as a counterstain.

OA grading and scoring

Serial sagittal histological sections of individual mouse knee joints were examined for signs of OA in a double-blind fashion. The slides were scored for OA severity used a grading system based upon the criteria of Maier and Wilhelmi [32]. This system uses the following scale to quantify OA severity: grade 0 indicates no apparent changes, grade 1 indicates slight fibrillation of the articular cartilage, grade 2 specifies defects limited to the uncalcified cartilage, grade 3 specifies defects penetrating into the calcified cartilage, and grade 4 indicates subchondral bone exposure at the joint surface. Scores for each genotype were averaged and analyzed using an unpaired Student's t-test with Welch's and Bonferroni corrections.

RNA isolation, microarray hybridization, and data analysis

Males were chosen for these experiments because they displayed increased joint disease severity as compared to females. *Epn/Bgn* double-deficient and wild type mice were sacrificed at three months of age ($n = 3$ for each genotype). The tibial-femoral joints of each male mouse were harvested by dissecting the joint immediately above the femoral condyles and immediately below the tibial plateau, measuring approximately 1 cm in length. Skin,

tendons, and ligaments around the joint were removed for reproducibility of the procedure. The joint tissue was then immediately frozen in liquid nitrogen and pooled for RNA isolation (for a total of 6 joints per genotype). Total RNA was isolated using TRIzol®-mediated organic extraction (Invitrogen, Carlsbad, CA) followed by purification with RNeasy mini columns (Qiagen, Valencia, CA) according to the manufacturer's instructions. RNA integrity was assessed using formaldehyde gel electrophoresis.

Second-strand cDNA was generated from 5 μg of joint tissue RNA using an oligo(dT)-T7 promoter primer and SuperScript™ II reverse transcriptase (Invitrogen, Carlsbad, CA). cRNA was amplified from the cDNA and biotinylated using the BioArray™ High Yield™ RNA Transcript Labeling Kit (ENZO, Farmingdale, NY) according to the manufacturer's instructions. After purification, labeled cRNA was quantified using a spectrophotometer and fragmented in 200 mM Tris/acetate (pH 8.1), 500 mM potassium acetate, and 150 mM magnesium acetate for 35 min at 94°C. The fragmented cRNA was then hybridized overnight to the Mouse Genome 430A 2.0 GeneChip (Affymetrix, Santa Clara, CA). The resultant signal was detected according to the manufacturer's instructions. This procedure was repeated three times for each genotype; a different cRNA preparation was used for each hybridization event. All six arrays were analyzed using the dChip software package (www.dchip.org). Each array had a different level of overall brightness; the dChip program was therefore used to normalize arrays to the median intensity level using an invariant-set normalization method [33]. After normalization, expression values were calculated using a perfect match model [34]. The program parameters were set such that expression values at least 1.25-fold and an absolute difference of more than 100 between wild type and double-deficient samples were detected.

RESULTS

Generation and initial characterization of Epn-deficient mice

The *Epn* locus was disrupted in mouse embryonic stem cells by inserting a targeting vector into exon III downstream of the endogenous *Epn* translation start codon (Fig. 1A). Southern blot analysis verified that the *Epn* locus was correctly targeted, generating bands of the predicted fragment size (Fig. 1B and C). The genotypes of the mice were confirmed using PCR (Fig. 1D). Homozygous *Epn*-deficient mice were born with the expected Mendelian ratio, appeared healthy at birth, and were fertile. LacZ activity was not detected in the mutant embryos for unknown reasons.

Epn protein was undetectable in *Epn*-deficient mice at any age (Fig. 2A). In contrast, Epn protein was observed in wild type newborn mice within the ECM of all cartilaginous zones except the cartilage immediately adjacent to the joint cavitation space and the perichondrium (data not shown; [1]). At two weeks of age, Epn was detected in the deep layer of articular cartilage of wild type mice, but not within the superficial layer (Fig. 2B). Epn was also detected in growth plate cartilage. Very weak Epn staining was observed in the growth plate cartilage of two month old wild type mice (Fig. 2C). Epn protein was not detected in wild type mice older than two months (data not shown). The distribution of Epn protein in *Bgn*-deficient mice was similar to that described above for wild type mice (data not shown). Control sections from wild type mice where the anti-Epn antibody (R561) was omitted from the staining procedure showed no background (data not shown).

The localization of Epn protein within the tibial-femoral joint strongly resembles the localization of another SLRP, biglycan (Fig. 2D). Since biglycan genetically interacts with another SLRP molecule, fibromodulin [35], *Epn*-deficient mice were bred with biglycan (*Bgn)*-deficient mice to test whether biglycan genetically interacts with epiphycan. Similar

to *Epn*-deficient mice, *Epn/Bgn*-deficient mice were born in the expected Mendelian ratio, appeared healthy at birth, and were fertile.

Body weight and femur length

Due to the fact that Epn and Bgn are expressed in the cartilage growth plate of long bones, we examined the body weights and femur lengths of our SLRP-deficient mice. No significant difference in body weight was detected between the different genotypes at one month of age, regardless of gender (Fig. 3). At nine months, the body weights of male *Epn*- and *Bgn*-deficient mice were also similar to their wild type littermates. However, nine month old male *Epn/Bgn* double-deficient mice were significantly lighter by 17.1% ($p < 0.001$). No significant difference in body weight was detected between nine month old wild type and *Epn*-deficient females. However, the body weights of both *Bgn*- and *Epn/Bgn*-deficient females were 16.3% lighter than their wild type littermates at nine months ($p < 0.001$).

Next, the ability of Epn and/or Bgn to influence the growth of long bones was examined. The average femur length of one month old *Epn*-, *Bgn*-, or *Epn/Bgn* double-deficient mice was not significantly different than the average femur length of wild type mice, regardless of the gender. However, the femur lengths of nine month old male *Epn*- and *Epn/Bgn* double-deficient mice were significantly shorter than their wild type littermates by 3.9% ($p<0.05$) and 7.1% ($p<0.001$), respectively. Male *Bgn*-deficient femurs were not significantly shorter than wild type at this age. For females, only *Epn/Bgn* double-deficient femurs were significantly shorter than wild type at nine months (by 7%, $p< 0.001$).

Histology

To further assess joint tissue morphology and proteoglycan content, histological sections of tibial-femoral joints from four nine month old animals per genotype were characterized by hematoxylin/eosin and Safranin O staining. Histological evidence of premature OA was not observed in joint sections from wild type mice (Fig. 4A). However, osteoarthritic signs were observed in two of the four *Epn*-deficient mice, including articular surface fibrillations and significant proteoglycan loss (Fig. 4B). Similar observations were made in three of the four *Bgn*-deficient mice examined (Fig. 4C). The *Bgn*-deficient mice also showed evidence of ligament and tendon ossification (data not shown), in agreement with Ameye *et al.* [36]. The most severe OA-like phenotype was observed in *Epn/Bgn* double-deficient animals (Fig. 4D); joint sections from all four animals showed damaged articular cartilage that was often completely eroded to the underlying bone, which was typically sclerotic. *Epn/Bgn* double-deficient mice showed increased osteophyte formation within and around the joint space. Increased ligament and tendon ossification was also detected in these mice (data not shown).

To quantify the observed OA-like changes detected in our SLRP-deficient mice, histological sections of tibial-femoral joints from male mice of each genotype at various ages were examined in a double-blind fashion and scored using the OA grading system devised by Maier and Wilhelmi [32]. Compared to wild type mice, a number of the *Epn*- and *Bgn*-deficient mice began to display OA-like changes at six and four months of age, respectively (Fig. 5). *Epn/Bgn* double-deficient mice appeared to develop OA-like characteristics even sooner, as early as three months. Additionally, the OA grade in double-deficient mice was highly significant at six months, three months earlier than *Bgn*-deficient mice. *Epn*-deficient mice displayed OA-like changes that were only of borderline significance at nine months of age. Significant OA-like changes were also detected in female *Epn/Bgn* double-deficient mice, although these were less severe (data not shown).

Collagen content analysis

Since OA is associated not only with aggrecan but also collagen loss, we examined histological sections of male tibia-femoral joints for total collagen content using van Gieson stain at two, three, and six months. A difference in collagen staining when compared to wild type mice was detected within the superficial zone of articular cartilage in *Bgn*-deficient and *Epn/Bgn*-deficient mice as early as three months (Fig. 6). Collagen loss consistently appeared to be more pronounced at the articular surface of *Epn/Bgn* double-deficient mice when compared to *Bgn*-deficient mice (Fig. 6 inset). This was accompanied by a deficiency of superficial chondrocytes. *Epn*-deficient mice showed similar collagen staining when compared to wild type mice data not shown).

Microarray analysis

To examine what happens at the molecular level before significant OA-like morphological changes occur, we compared the mRNA profile of whole knee joints from three month old wild type and *Epn/Bgn* double-deficient male mice. We chose to analyze changes in the whole joint for two reasons: (1) OA is a disease of the whole joint and (2) In our experience, it is extremely difficult to obtain mouse cartilage samples that are not contaminated with other tissues, such as subchondral bone.

We detected a significant increase in the mRNA of 49 separate genes within *Epn/Bgn* double-deficient mice as compared to wild type mice. A total of 7 specific mRNAs were significantly decreased at this time point in the disease progression; the largest decrease detected was for Bgn (further confirmation that the mice were *Bgn*-deficient; Epn is not expressed at this age in wild type mice). The majority of mRNAs that were increased in double-deficient mice corresponded to secreted proteins. Of the genes encoding ECM proteins, the α1 chain of type III procollagen showed the largest increase (Table 1). The metalloproteinases MMP-2 and MMP-14, as well as the serine protease HtrA1, were also increased in *Epn/Bgn* double-deficient mice. Interestingly, three other SLRPs (asporin, fibromodulin, and lumican) were significantly up-regulated in double-deficient mice. A complete description of all the gene changes can be found in the NCBI Gene Expression Omnibus (GSE9099).

DISCUSSION

We previously showed that Epn has a highly restricted expression pattern within cartilage [1], suggesting that it plays a role in skeletal formation and/or maintenance. The generation of *Epn*-deficient mice demonstrated that although Epn is not essential for embryonic skeletal development, it is critical for proper long bone growth and joint maintenance. For example, Epn significantly influences femur length in male mice. This effect is presumably due to subtle defects in the growth plate since Epn is not expressed in bone. Furthermore, Epn is necessary for retaining cartilage integrity with age because Epn loss, in the absence of Bgn, significantly accelerates the rate of OA-like lesion development when compared to their single SLRP-deficient littermates. The rapid progression of OA in the double-deficient mouse suggests one of two possibilities: (1) Epn and Bgn have some overlapping functions within cartilage or (2) Epn and Bgn have independent functions that, when deleted, exacerbate the progression of OA. Future work will be necessary to demonstrate which possibility is correct. Nevertheless, our data are the first to show an *in vivo* genetic interaction involving class I and class III SLRPs.

Our collagen content analysis in the tibia-femoral joints of SLRP-deficient animals demonstrated that collagen loss occurred at the articular cartilage surface in both *Bgn*-deficient and *Epn/Bgn* double-deficient mice. However, collagen loss appeared to be greater

in *Epn/Bgn* double-deficient animals. These data imply that Epn influences the stability of the collagen matrix in a *Bgn*- deficient background, again suggesting that Bgn and Epn share a function in maintaining joint integrity. Collagen loss in mutant animals preceded significant OA-like changes as measured by the Maier and Whilhelmi OA grading scale and may therefore be responsible for increasing their susceptibility to develop OA. In human osteoarthritic cartilage samples, collage degradation [37] and loss of collagen tensile strength [38] is detected early in the disease. Interestingly, increased collagen degradation has been observed either before [37] or at a similar time as proteoglycan loss [39]. Future studies to investigate whether this apparent loss of collagen staining is due to increased collagen degradation are underway.

Epn/Bgn double-deficient mice are not the only SLRP-deficient mice that develop OA-like changes. Previous work has shown that *Bgn*-deficient [35], fibromodulin-deficient [40], *Bgn*/fibromodulin double-deficient [35], and lumican/fibromodulin double-deficient mice [16] also develop an OA-like disease. In all of the cases examined thus far, the double-deficient mice develop OA earlier than their single SLRP-deficient counterparts, demonstrating the necessity for multiple SLRPs to maintain joint integrity. The SLRP-mutants described above also show tendon abnormalities that likely contribute toward OA development and/or progression.

We currently do not know why the absence of a protein that is apparently expressed only early in life, such as Epn, would show effects later in life. However, there are several possible explanations. Firstly, Epn could be required for stabilizing the cartilage matrix through its ability to influence collagen fibrillogenesis, matrix assembly, or chondrocyte-ECM interactions. The fact that other SLRPs are known to influence collagen fibril formation and our collagen content analysis support this possibility. Secondly, Epn may influence one or more currently undefined cell signaling events that are necessary for proper chondrocyte/cartilage maintenance. This idea is supported by the recent work of Schaefer *et al*. [41], where Bgn was shown to signal through TLR-2 and TLR-4. Thirdly, Epn may be required for repairing localized joint damage. In this scenario, a currently undetectable, localized expression of Epn by chondrocytes possibly helps to repair matrix defects that accumulate throughout life. Fourthly, Epn may directly or indirectly influence the structure of the subchondral bone matrix. Epn loss would therefore lead to cartilage degeneration because of the altered subchondral bone structure. The answer may also be a combination of the possibilities listed above.

We also do not know the reason behind the gender differences reported herein. For example, femurs are significantly shorter in male but not female *Epn*-deficient mice when compared to wild type mice. Sex hormone and/or body weight differences may play a role. However, future work is needed to fully understand these effects. Generally speaking, gender differences in genetically-manipulated mice are not well studied, although there a few examples reported in the literature (e.g. *Bgn/Fibromodulin*-deficient mice [35] and estrogen receptor-β knockout mice [42]).

Interestingly, our microarray analysis of *Epn/Bgn* double-deficient mice detected increased ECM gene expression that can also be seen in human OA samples [43–46]. These include the mRNAs of the type III collagen α chain [43,45], matrix metalloproteinase 2 [43,45], fibronectin [43,45,46], lumican [47], and fibromodulin [47]. Furthermore, we detected increases in mRNAs that are known to be increased at the protein level in human osteoarthritic cartilage, including type VI collagen protein [48], annexin VIII protein [49], and insulin-like growth factor 1 protein [50]. However, our microarray data also suggests that superoxide dismutase 3 is increased in *Epn/Bgn* double-deficient tissue; this protein has actually been shown to be decreased in human osteoarthritic cartilage and in a naturally

occurring OA mouse model, STR/ort [51]. This discrepancy may be due to the fact that the tissues are not identical (whole joints vs. cartilage alone).

Of interest, the mRNA levels of three different SLRPs (asporin, fibromodulin, and lumican) are increased in *Epn/Bgn* double-deficient mice as compared with wild type mice. These data suggest that the expression of various SLRPs are somehow interrelated and may be further proof of the ability of SLRP molecules to compensate for each other.

Taken together, the data presented herein suggests that *Epn/Bgn* double-deficient mice may be a useful tool for the study of OA. The tibia-femoral joints from *Epn/Bgn* double-deficient mice show similar morphological changes to human OA joints, including articular cartilage erosions, proteoglycan loss, subchondral bone sclerosis, and osteophyte growth. While our deficient mice are not the only OA murine model to be proposed, their usefulness lies in the fact that significant characteristics of the disease are detected fairly quickly (by 6 months) with complete penetrance. Furthermore, our model has the potential to shed light on how SLRPs influence the molecular events that lead to OA. The fact that many different genetic and physical manipulations in mice cause an OA-like phenotype suggests that joint health is maintained by a variety of factors. Since human OA is thought to be a multifactorial disease, we believe that the use of multiple murine models, including SLRP-deficient mice, is necessary to best understand the disease progression.

Acknowledgments

FUNDING SOURCES

This work was supported by NIH grants P01AR042919 and R01AR047433.

References

1. Johnson J, Shinomura T, Eberspaecher H, Pinero G, Decrombrugghe B, Hook M. Expression and localization of PG-Lb/epiphycan during mouse development. Dev Dyn 1999;216:499–510. [PubMed: 10633869]
2. Roughley PJ. The structure and function of cartilage proteoglycans. Eur Cell Mater 2006;12:92–101. [PubMed: 17136680]
3. Schmidt G, Robenek H, Harrach B, Glossl J, Nolte V, Hormann H, et al. Interaction of small dermatan sulfate proteoglycan from fibroblasts with fibronectin. J Cell Biol 1987;104:1683–1691. [PubMed: 3584245]
4. Winnemoller M, Schon P, Vischer P, Kresse H. Interactions between thrombospondin and the small proteoglycan decorin: interference with cell attachment. Eur J Cell Biol 1992;59:47–55. [PubMed: 1468447]
5. Dugan TA, Yang VW, McQuillan DJ, Hook M. Decorin modulates fibrin assembly and structure. J Biol Chem. 2006
6. Whinna HC, Choi HU, Rosenberg LC, Church FC. Interaction of heparin cofactor II with biglycan and decorin. J Biol Chem 1993;268:3920–3924. [PubMed: 8440685]
7. Krumdieck R, Hook M, Rosenberg LC, Volanakis JE. The proteoglycan decorin binds C1q and inhibits the activity of the C1 complex. J Immunol 1992;149:3695–3701. [PubMed: 1431141]
8. Sjoberg A, Onnerfjord P, Morgelin M, Heinegard D, Blom AM. The extracellular matrix and inflammation: fibromodulin activates the classical pathway of complement by directly binding C1q. J Biol Chem 2005;280:32301–32308. [PubMed: 16046396]
9. Hocking AM, Strugnell RA, Ramamurthy P, McQuillan DJ. Eukaryotic expression of recombinant biglycan. Post-translational processing and the importance of secondary structure for biological activity. J Biol Chem 1996;271:19571–19577. [PubMed: 8702651]

10. Groeneveld TW, Oroszlan M, Owens RT, Faber-Krol MC, Bakker AC, Arlaud GJ, et al. Interactions of the extracellular matrix proteoglycans decorin and biglycan with C1q and collectins. J Immunol 2005;175:4715–4723. [PubMed: 16177119]
11. Nadesalingam J, Bernal AL, Dodds AW, Willis AC, Mahoney DJ, Day AJ, et al. Identification and characterization of a novel interaction between pulmonary surfactant protein D and decorin. J Biol Chem 2003;278:25678–25687. [PubMed: 12730206]
12. Hildebrand A, Romaris M, Rasmussen LM, Heinegard D, Twardzik DR, Border WA, et al. Interaction of the small interstitial proteoglycans biglycan, decorin and fibromodulin with transforming growth factor beta. Biochem J 1994;302 (Pt 2):527–534. [PubMed: 8093006]
13. Yamaguchi Y, Mann DM, Ruoslahti E. Negative regulation of transforming growth factor-beta by the proteoglycan decorin. Nature 1990;346:281–284. [PubMed: 2374594]
14. Iozzo RV. The biology of the small leucine-rich proteoglycans. Functional network of interactive proteins. J Biol Chem 1999;274:18843–18846. [PubMed: 10383378]
15. Chakravarti S, Magnuson T, Lass JH, Jepsen KJ, LaMantia C, Carroll H. Lumican regulates collagen fibril assembly: skin fragility and corneal opacity in the absence of lumican. J Cell Biol 1998;141:1277–1286. [PubMed: 9606218]
16. Jepsen KJ, Wu F, Peragallo JH, Paul J, Roberts L, Ezura Y, et al. A syndrome of joint laxity and impaired tendon integrity in lumican- and fibromodulin-deficient mice. J Biol Chem 2002;277:35532–35540. [PubMed: 12089156]
17. Svensson L, Narlid I, Oldberg A. Fibromodulin and lumican bind to the same region on collagen type I fibrils. FEBS Lett 2000;470:178–182. [PubMed: 10734230]
18. Aigner T, Fundel K, Saas J, Gebhard PM, Haag J, Weiss T, et al. Large-scale gene expression profiling reveals major pathogenetic pathways of cartilage degeneration in osteoarthritis. Arthritis Rheum 2006;54:3533–3544. [PubMed: 17075858]
19. Monfort J, Tardif G, Roughley P, Reboul P, Boileau C, Bishop PN, et al. Identification of opticin, a member of the small leucine-rich repeat proteoglycan family, in human articular tissues: a novel target for MMP-13 in osteoarthritis. Osteoarthritis Cartilage. 2007
20. Lorenzo P, Aspberg A, Onnerfjord P, Bayliss MT, Neame PJ, Heinegard D. Identification and characterization of asporin. a novel member of the leucine-rich repeat protein family closely related to decorin and biglycan. J Biol Chem 2001;276:12201–12211. [PubMed: 11152692]
21. Bengtsson E, Neame PJ, Heinegard D, Sommarin Y. The primary structure of a basic leucine-rich repeat protein, PRELP, found in connective tissues. J Biol Chem 1995;270:25639–25644. [PubMed: 7592739]
22. Corpuz LM, Funderburgh JL, Funderburgh ML, Bottomley GS, Prakash S, Conrad GW. Molecular cloning and tissue distribution of keratocan. Bovine corneal keratan sulfate proteoglycan 37A. J Biol Chem 1996;271:9759–9763. [PubMed: 8621655]
23. Neame PJ, Sommarin Y, Boynton RE, Heinegard D. The structure of a 38-kDa leucine-rich protein (chondroadherin) isolated from bovine cartilage. J Biol Chem 1994;269:21547–21554. [PubMed: 8063792]
24. Cs-Szabo G, Roughley PJ, Plaas AH, Glant TT. Large and small proteoglycans of osteoarthritic and rheumatoid articular cartilage. Arthritis Rheum 1995;38:660–668. [PubMed: 7538297]
25. Jiang Q, Shi D, Yi L, Ikegawa S, Wang Y, Nakamura T, et al. Replication of the association of the aspartic acid repeat polymorphism in the asporin gene with knee-osteoarthritis susceptibility in Han Chinese. J Hum Genet 2006;51:1068–1072. [PubMed: 17024313]
26. Kizawa H, Kou I, Iida A, Sudo A, Miyamoto Y, Fukuda A, et al. An aspartic acid repeat polymorphism in asporin inhibits chondrogenesis and increases susceptibility to osteoarthritis. Nat Genet 2005;37:138–144. [PubMed: 15640800]
27. Kurita K, Shinomura T, Ujita M, Zako M, Kida D, Iwata H, et al. Occurrence of PG-Lb, a leucine-rich small chondroitin/dermatan sulphate proteoglycan in mammalian epiphyseal cartilage: molecular cloning and sequence analysis of the mouse cDNA. Biochem J 1996;318 (Pt 3):909–914. [PubMed: 8836137]
28. Shinomura T, Kimata K. Proteoglycan-Lb, a small dermatan sulfate proteoglycan expressed in embryonic chick epiphyseal cartilage, is structurally related to osteoinductive factor. J Biol Chem 1992;267:1265–1270. [PubMed: 1730648]

29. Xu T, Bianco P, Fisher LW, Longenecker G, Smith E, Goldstein S, et al. Targeted disruption of the biglycan gene leads to an osteoporosis-like phenotype in mice. Nat Genet 1998;20:78–82. [PubMed: 9731537]
30. Ramirez-Solis R, Rivera-Perez J, Wallace JD, Wims M, Zheng H, Bradley A. Genomic DNA microextraction: a method to screen numerous samples. Anal Biochem 1992;201:331–335. [PubMed: 1632522]
31. Fisher LW, Stubbs JT 3rd, Young MF. Antisera and cDNA probes to human and certain animal model bone matrix noncollagenous proteins. Acta Orthop Scand Suppl 1995;266:61–65. [PubMed: 8553864]
32. Maier R, Wilhelmi G. Evaluation of the effect of analgesics/antiphlogistics on the progression of spontaneous arthrosis in the C57 black mouse. Z Rheumatol 1983;42:232–234. [PubMed: 6649933]
33. Li C, Hung Wong W. Model-based analysis of oligonucleotide arrays: model validation, design issues and standard error application. Genome Biol 2001;2:RESEARCH0032. [PubMed: 11532216]
34. Li C, Wong WH. Model-based analysis of oligonucleotide arrays: expression index computation and outlier detection. Proc Natl Acad Sci U S A 2001;98:31–36. [PubMed: 11134512]
35. Ameye L, Aria D, Jepsen K, Oldberg A, Xu T, Young MF. Abnormal collagen fibrils in tendons of biglycan/fibromodulin-deficient mice lead to gait impairment, ectopic ossification, and osteoarthritis. Faseb J 2002;16:673–680. [PubMed: 11978731]
36. Ameye L, Young MF. Mice deficient in small leucine-rich proteoglycans: novel in vivo models for osteoporosis, osteoarthritis, Ehlers-Danlos syndrome, muscular dystrophy, and corneal diseases. Glycobiology 2002;12:107R–116R.
37. Dodge GR, Poole AR. Immunohistochemical detection and immunochemical analysis of type II collagen degradation in human normal, rheumatoid, and osteoarthritic articular cartilages and in explants of bovine articular cartilage cultured with interleukin 1. J Clin Invest 1989;83:647–661. [PubMed: 2783591]
38. Kempson GE, Muir H, Pollard C, Tuke M. The tensile properties of the cartilage of human femoral condyles related to the content of collagen and glycosaminoglycans. Biochim Biophys Acta 1973;297:456–472. [PubMed: 4267503]
39. Hollander AP, Pidoux I, Reiner A, Rorabeck C, Bourne R, Poole AR. Damage to type II collagen in aging and osteoarthritis starts at the articular surface, originates around chondrocytes, and extends into the cartilage with progressive degeneration. J Clin Invest 1995;96:2859–2869. [PubMed: 8675657]
40. Gill MR, Oldberg A, Reinholt FP. Fibromodulin-null murine knee joints display increased incidences of osteoarthritis and alterations in tissue biochemistry. Osteoarthritis Cartilage 2002;10:751–757. [PubMed: 12359160]
41. Schaefer L, Babelova A, Kiss E, Hausser HJ, Baliova M, Krzyzankova M, et al. The matrix component biglycan is proinflammatory and signals through Toll-like receptors 4 and 2 in macrophages. J Clin Invest 2005;115:2223–2233. [PubMed: 16025156]
42. Sims NA, Dupont S, Krust A, Clement-Lacroix P, Minet D, Resche-Rigon M, et al. Deletion of estrogen receptors reveals a regulatory role for estrogen receptors-beta in bone remodeling in females but not in males. Bone 2002;30:18–25. [PubMed: 11792560]
43. Aigner T, Zien A, Gehrsitz A, Gebhard PM, McKenna L. Anabolic and catabolic gene expression pattern analysis in normal versus osteoarthritic cartilage using complementary DNA-array technology. Arthritis Rheum 2001;44:2777–2789. [PubMed: 11762938]
44. Aigner T, Zien A, Hanisch D, Zimmer R. Gene expression in chondrocytes assessed with use of microarrays. J Bone Joint Surg Am 2003;85-A(Suppl 2):117–123. [PubMed: 12721354]
45. Gebauer M, Saas J, Haag J, Dietz U, Takigawa M, Bartnik E, et al. Repression of anti-proliferative factor Tob1 in osteoarthritic cartilage. Arthritis Res Ther 2005;7:R274–284. [PubMed: 15743474]
46. Sato T, Konomi K, Yamasaki S, Aratani S, Tsuchimochi K, Yokouchi M, et al. Comparative analysis of gene expression profiles in intact and damaged regions of human osteoarthritic cartilage. Arthritis Rheum 2006;54:808–817. [PubMed: 16508957]

47. Cs-Szabo G, Melching LI, Roughley PJ, Glant TT. Changes in messenger RNA and protein levels of proteoglycans and link protein in human osteoarthritic cartilage samples. Arthritis Rheum 1997;40:1037–1045. [PubMed: 9182913]

48. Hambach L, Neureiter D, Zeiler G, Kirchner T, Aigner T. Severe disturbance of the distribution and expression of type VI collagen chains in osteoarthritic articular cartilage. Arthritis Rheum 1998;41:986–996. [PubMed: 9627008]

49. White AH, Watson RE, Newman B, Freemont AJ, Wallis GA. Annexin VIII is differentially expressed by chondrocytes in the mammalian growth plate during endochondral ossification and in osteoarthritic cartilage. J Bone Miner Res 2002;17:1851–1858. [PubMed: 12369789]

50. Schneiderman R, Rosenberg N, Hiss J, Lee P, Liu F, Hintz RL, et al. Concentration and size distribution of insulin-like growth factor-I in human normal and osteoarthritic synovial fluid and cartilage. Arch Biochem Biophys 1995;324:173–188. [PubMed: 7503553]

51. Regan E, Flannelly J, Bowler R, Tran K, Nicks M, Carbone BD, et al. Extracellular superoxide dismutase and oxidant damage in osteoarthritis. Arthritis Rheum 2005;52:3479–3491. [PubMed: 16255039]

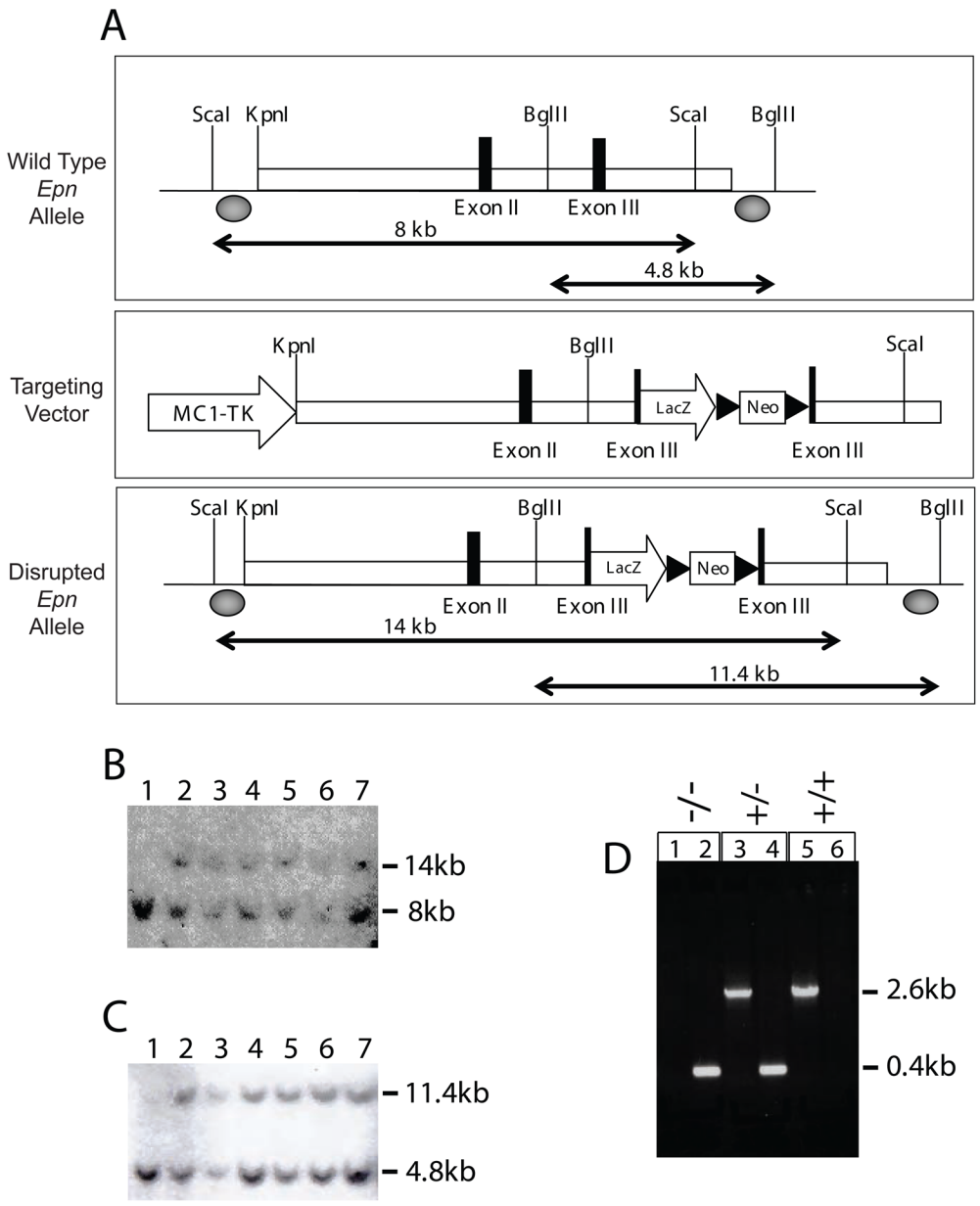

Figure 1. Generation of *Epn*-deficient mice

A, At the top is a schematic representation of the partial *Epn* gene locus; in the middle is the targeting vector created to disrupt the *Epn* gene; at the bottom is the final product with the disrupted *Epn* allele. *B*, Mouse ES cell genomic DNA digested with ScaI and subjected to Southern blot analysis. The radiolabeled 5' probe detects an 8 kb fragment from the wild type *Epn* allele and a 14 kb fragment from the interrupted *Epn* allele. Lane 1 is an untargeted ES clone and lanes 2-7 are targeted ES clones. *C*, Mouse ES cell genomic DNA digested with BglII and subjected to Southern blot analysis. The radiolabeled 3' probe detects a 4.8 kb fragment from the wild type *Epn* allele and an 11.4 kb fragment from the interrupted *Epn* allele. Lane 1 is an untargeted ES clone and lanes 2-7 are targeted ES clones.*D*, Genotyping of the mice. A 2.6 kb fragment is amplified from the wild type Epn allele with the primer pair Epnlfw/Epn2rv (lanes 3 and 5), whereas a 0.4 kb fragment is amplified from the interrupted *Epn* allele with the primer pair Bpa/Epn2rv (lanes 2 and 4).

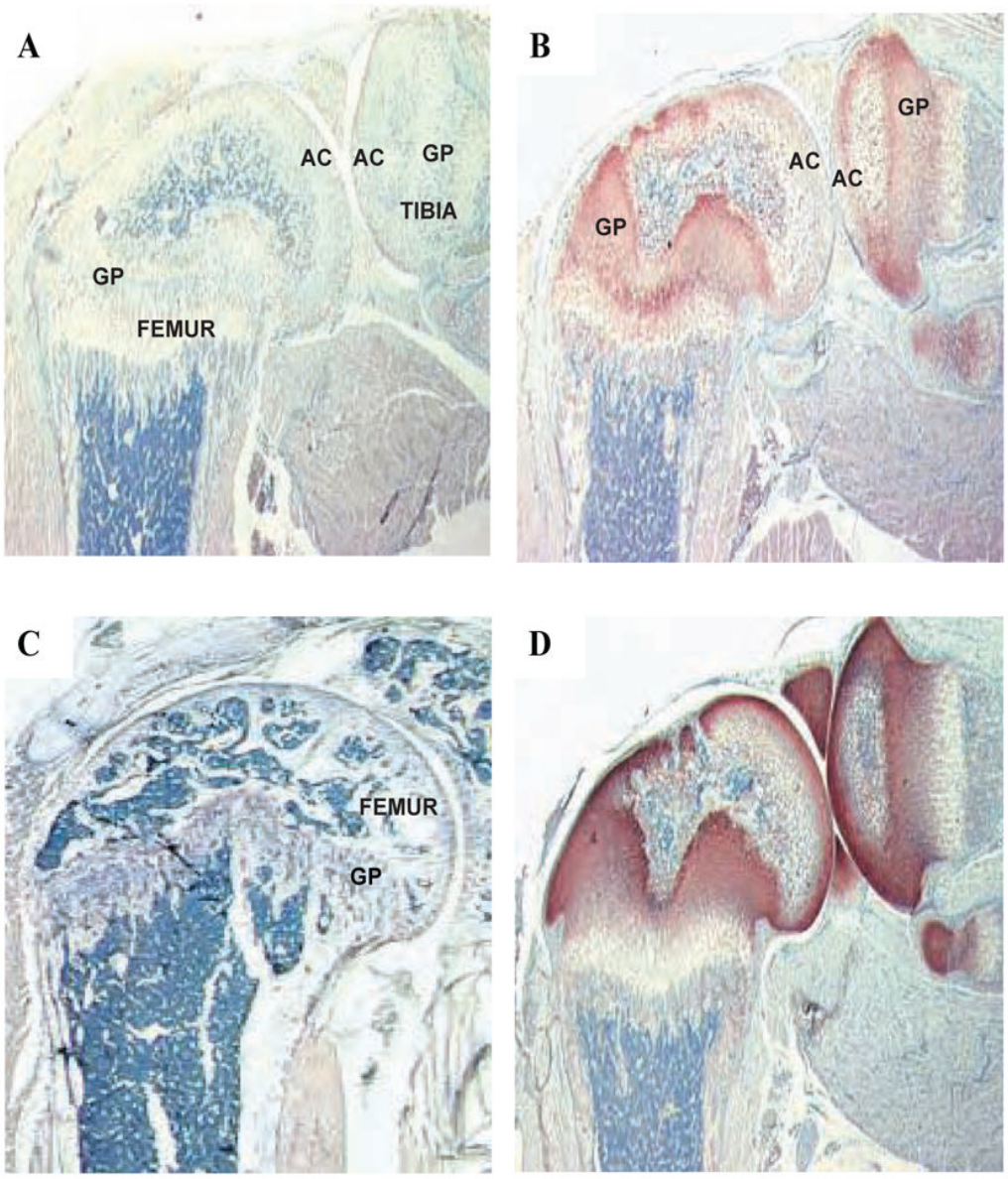

Figure 2. Immunohistological analysis of murine knee joints using the anti- Epn antibody, R561, or the anti-Bgn antibody, LF-159

Panels A, B, and D are oriented in the same manner, with the femur on the left and the tibia on the right. *A*, R561 antibody staining of a 2-week-old *Epn*-deficient tibia-femoral joint. AC = articular cartilage and GP = growth plate. *B*, R561 antibody staining of a 2- week-old wild type tibia-femoral joint. Epn is detected in the growth plate and articular cartilage. *C*, R561 antibody staining of a 2-month-old wild type femur showing very weak expression of Epn protein in the growth plate. *D*, LF-159 antibody staining of a 2-week-old wild type tibia-femoral joint. Bgn is detected in the growth plate, articular cartilage, and the meniscus.

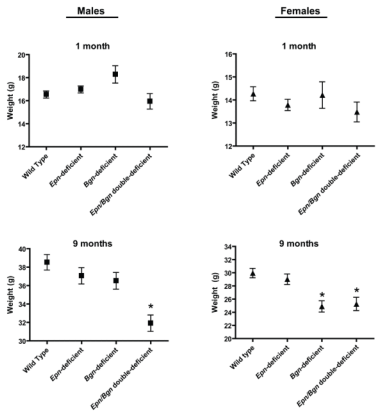

Figure 3. Mean body weights of wild type and SLRP-deficient mice at 1 and 9 months of age
The asterisks denote a significant difference in body weight as compared to wild type mice ($p<0.001$). The error bars denote the SEM for each genotype.

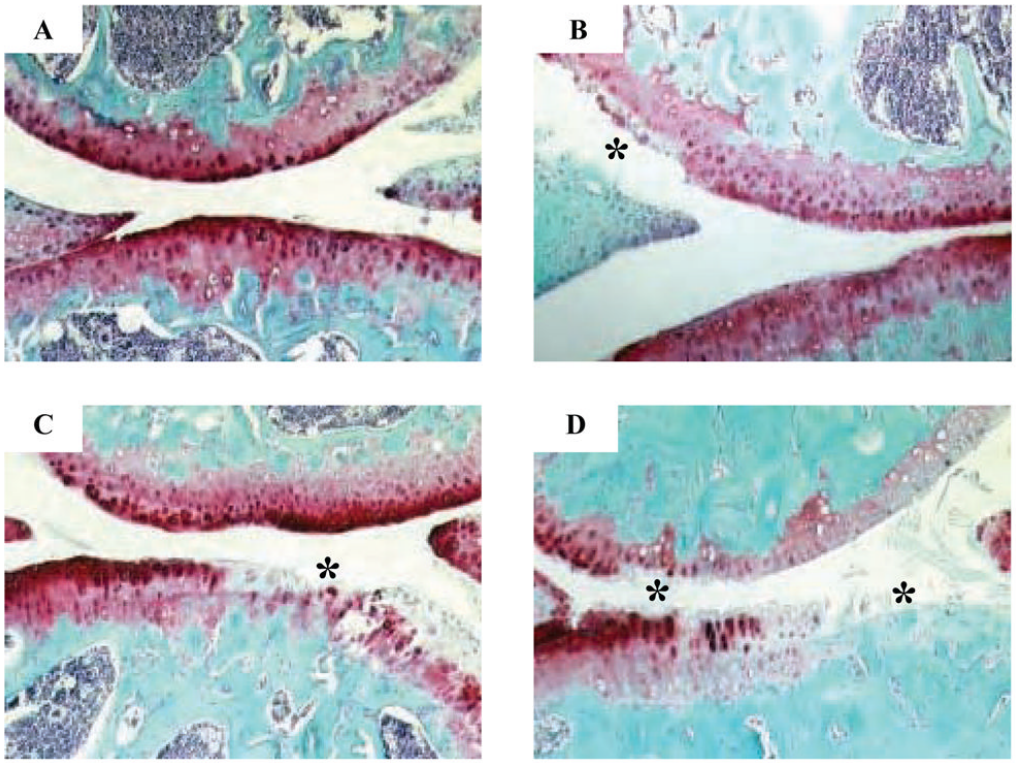

Figure 4. Safranin O staining of the tibia-femoral joint in 9 month old mice

In each panel, the femur is at the top and the tibia is at the bottom of the picture. *A*, Representative joint section from a wild type animal. *B*, Representative joint section from an *Epn*-deficient mouse. *C*, Representative joint section from a *Bgn*-deficient mouse. *D*, Representative joint section from an *Epn/Bgn* double-deficient mouse. The asterisks in panels *B*, *C*, *and D* denote fibrillation as well as articular cartilage and proteoglycan loss.

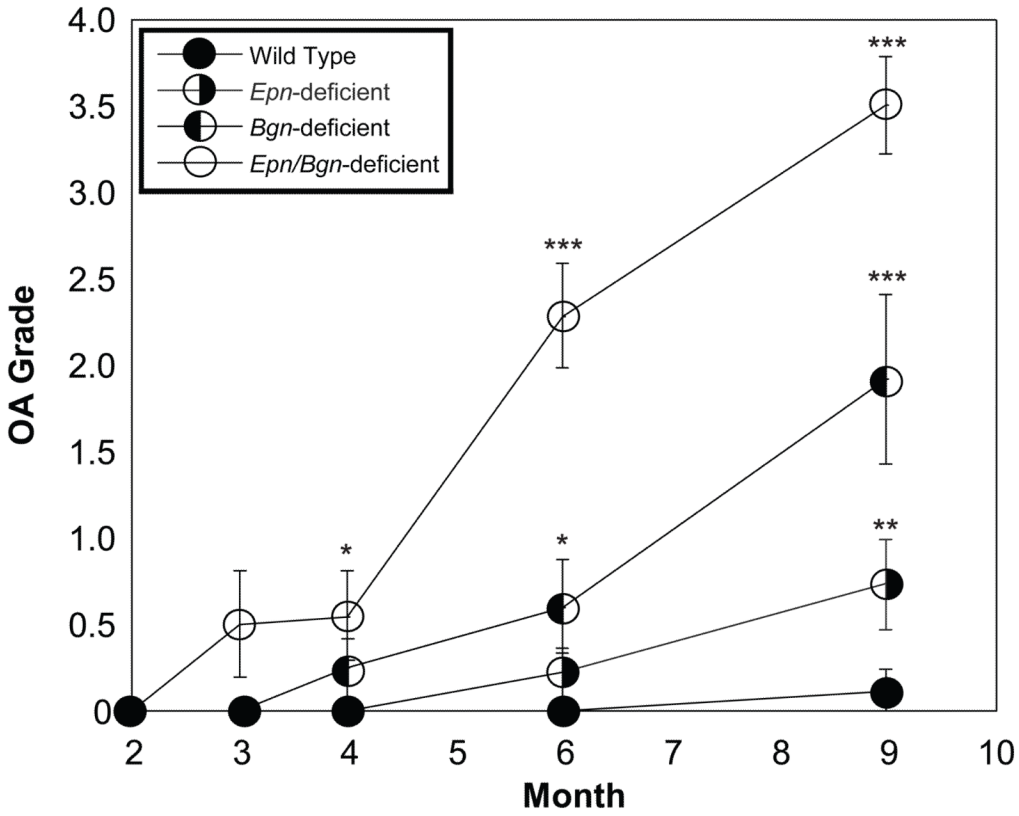

Figure 5. Mean scores of OA severity in male wild type and SLRP-deficient mice

Sections of the tibia-femoral joint in wild-type, *Epn*-deficient, *Bgn*-deficient, and *Epn/Bgn* double-deficient mice were scored for OA using the criteria of Maier and Wilhelmi (30). A minimum of 4 mice were examined at every age for each genotype. The age of the mice in months is given on the x-axis, while the OA grade is shown on the y-axis. The error bars denote the SEM for each genotype. * $p \leq 0.053$, ** $p = 0.036$, and *** $p < 0.005$ compared to wild type mice at that age. With Bonferroni correction, a p value of ≤0.02 is necessary to reach statistical significance.

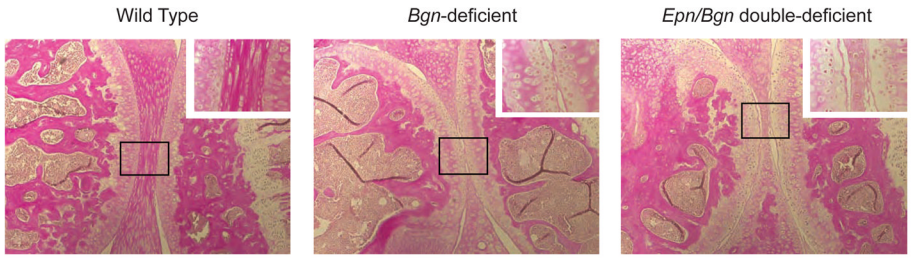

Figure 6. Collagen analysis in tibia-femoral joints

Sections of 3 month old male mouse tibia-femoral joints from wild type, *Bgn*-deficient, and *Epn/Bgn* double-deficient mice were stained with van Giesen to analyze collagen content. The image at the top left of each panel is a 6-fold magnified image of the area denoted by the black box ($n = 3$).

Table 1

Genes of proteins found in the ECM that are regulated in *Epn/Bgn* double-deficient mice

	3-month-old *Epn/Bgn* deficient vs. WT
Gene	Fold Change
Procollagen, type III, α1	5.78
Asporin	3.07
Syndecan 2	2.69
Follistatin-like	2.67
Fibrillin 1	2.44
Dermatopontin	2.38
Superoxide dismutase 3, extracellular	2.35
Annexin VIII	2.32
Insulin-like growth factor 1	2.29
Procollagen, type VI, α1	2.26
Procollagen, type VI, α2	2.22
Lumican	2.12
HtrA1 peptidase	2.06
Fibromodulin	2.04
Procollagen, type VI, α3	1.92
Fibronectin 1	1.92
Procollagen C-proteinase enhancer protein	1.88
Matrix metalloproteinase 2	1.87
Thrombospondin 4	1.86
Procollagen, type V, α1	1.76
Procollagen, type IV, α2	1.63
Marix metalloproteinase 14	1.59
Biglycan	−36.07